

Electrically active deep levels formed by thermal oxidation of n-type 4H-SiC

Cite as: J. Appl. Phys. 125, 205302 (2019); doi: 10.1063/1.5090261

Submitted: 25 January 2019 · Accepted: 3 May 2019 ·

Published Online: 23 May 2019



L. Knoll, L. Kranz, and G. Alfieri^{a)}

AFFILIATIONS

ABB Corporate Research, Segelhofstrasse 1K, 5405 Baden-Dättwil, Switzerland

^{a)}Electronic mail: giovanni.alfieri@ch.abb.com

ABSTRACT

The doubly negative charge state of the carbon vacancy is a lifetime killer defect in n-type 4H-SiC. One way to reduce the concentration of this defect is by thermal oxidation. In this study, we electrically characterized n-type 4H-SiC epilayers that underwent dry thermal oxidation. While we confirm that the reduction of V_C is accompanied by the formation of the previously identified ON1 and ON2 levels, we additionally report on the presence of two new shallow levels. These are found at 0.19 and 0.24 eV below the conduction band edge. Their nature is discussed on the basis of their thermal stability and formation kinetics. The former was studied up to 1600 °C, whereas the latter was carried out by performing oxidation in the 1200–1300 °C temperature range and in the 45 min–24 h time range.

Published under license by AIP Publishing. <https://doi.org/10.1063/1.5090261>

I. INTRODUCTION

The double negative charge state of the carbon vacancy (V_C) in n-type 4H-SiC has a negative-U behavior; it is labeled $Z_{1/2}$ and is located at 0.6–0.7 eV below the conduction band edge (E_C).¹ This electrically active level is of great technological importance in 4H-SiC, as the presence of $Z_{1/2}$ was linked to the increase of leakage current and to the decrease of the minority carrier lifetime (τ) in electronic devices.^{2–4}

Since low τ has a negative effect on SiC bipolar devices, the scientific community has focused on ways to reduce $[Z_{1/2}]$: a base region with low $[Z_{1/2}]$ allows longer τ , which, in turn, leads to higher gain and to a smaller forward voltage drop. Until now, three methods are known for the reduction of $[Z_{1/2}]$. The first one is implantation-based:³ carbon atoms are implanted on the epilayer surface, and subsequent high-temperature annealing induces the diffusion of carbon interstitials (C_i). By diffusing C_i in the epilayer, it was shown that C_i recombined with V_C , thus leading to an increase of τ . The second method is oxidation-based.⁴ Since it was known that thermal oxidation causes injection of C_i ⁵ in the epilayer, Hiyoshi and Kimoto⁴ took advantage of this finding to successfully remove V_C throughout a thick epilayer, increasing τ . The third method, proposed by Ayedh *et al.*,⁶ is based on annealing of epilayers, at moderate temperatures (1500 °C) and in C-rich conditions, e.g., through the use of a carbon cap. Similarly to the other two, this method also relies on the injection of mobile C_i recombining with V_C .

The oxidation technique has several advantages compared to other methods. First, dry oxidation is performed at temperatures ranging between 1200 and 1400 °C and times can be adjusted according to the epilayer thickness.² Second, the high annealing temperatures needed for the second and third methods (≥ 1500 °C) require an extra processing step for the protection of the epilayer surface, which is not necessary when dry oxidation is used. Such protection, e.g., C-cap, must be removed after annealing by ashing or low temperature oxidation. Third, reactive ion etching (RIE) needs to be used for the removal of the implanted layer. For all these reasons, in the following, we will focus on the dry oxidation process only.

Despite being able to control τ , it was observed that the reduction of $[Z_{1/2}]$ is accompanied by the simultaneous formation of two new electrically active levels called ON1 and ON2.^{2,7} These are located at $E_C - 0.8$ eV and $E_C - 1.1$ eV. It was shown that the increase of the oxidation temperature, which is required for the faster and deeper removal of $Z_{1/2}$, causes the increase of both [ON1] and [ON2] (up to $\sim 10^{13}$ cm⁻³).² This, together with the fact that ON1 and ON2 are thermally stable up to 1700 °C,² has suggested that the nature of these two levels could be associated to C_i -related complex.² Despite the fact that ON1 and ON2 can reach rather high concentrations, it was found that their effect on the performance of electronic devices is limited, as they only behave as weak recombination centers.⁷

Besides controlling τ , dry oxidation is also used for gate oxides in MOSFETs. Since trapping of carriers in MOSFETs by defects in the semiconductor is equally important as that by oxide traps,⁸ and since studies on $Z_{1/2}$ removal have focused on the 0.5–1.6 eV energy range in the bandgap,^{2,4} it is straightforward to ask whether or not traps, other than ON1 and ON2, can arise during oxidation.

To clarify this issue, we present an electrical characterization study of an n-type 4H-SiC epilayer that underwent the $Z_{1/2}$ removal procedure in the 1200–1300 °C temperature range and for times ranging between 45 min and 24 h.

II. EXPERIMENTAL DETAILS

15 μm thick 4°-off n-type 4H-SiC epilayers (CREE) with a net-donor (N_d) concentration of $2\text{--}4 \times 10^{15} \text{ cm}^{-3}$, grown on the Si-face of a highly doped substrate (approximately 10^{18} cm^{-3}), were oxidized in a dry ambient. Some of the samples underwent a nitridation (N_2O) after dry oxidation. Prior to oxidation, samples were cleaned by employing Piranha solution. Dry oxidation was carried out at 1200, 1245, 1267, and 1290 °C for times ranging between 45 min and 24 h. After oxidation, samples were etched in diluted (5%) HF.

A separate set of as-grown or oxidized (and subsequently etched) samples was annealed for 600 min at 1290 °C or 30 min at 1600 °C, respectively, in an Ar atmosphere. Prior to annealing, a graphitic cap was formed on the epilayer surface. After annealing, capping was removed by O_2 ashing.

In order to carry out the electrical characterization, Ni Schottky contacts (1 mm diameter) were formed on the epilayer surface, by e-beam deposition, whereas Ag paste on the backside served as ohmic contact.

Samples were then electrically characterized by Fourier-transform deep level transient spectroscopy (FT-DLTS)⁹ in the 77–650 K temperature range, using a reverse bias (V_r) of -2 V a pulse voltage (V_p) of 2 V of the duration of 1 ms.

III. RESULTS AND DISCUSSION

In Fig. 1, the DLTS spectrum of the as-grown and as-grown plus dry oxidation samples is shown. Prior to oxidation [Fig. 1(a)], three DLTS peaks are clearly visible. One is found at $\sim 77 \text{ K}$ and

located at ($E_C - 0.16 \text{ eV}$, $8 \times 10^{11} \text{ cm}^{-3}$). This level bears close resemblance to the Ti impurity (at a cubic site) level reported in the literature by Dalibor *et al.*¹⁰ and by Ometoso *et al.*¹¹ The other two levels, at $\sim 300 \text{ K}$ and $\sim 650 \text{ K}$, correspond to the $Z_{1/2}$ (10^{12} cm^{-3}) and the $\text{EH}_{6/7}$, respectively, the two well-known charge states of V_C .

45 min dry oxidation at 1290° [Fig. 1(b)] results in the decrease of $[Z_{1/2}]$ to below the detection limit and in the formation of the ON1 ($3 \times 10^{12} \text{ cm}^{-3}$) and ON2 ($9 \times 10^{11} \text{ cm}^{-3}$) levels, while the Ti level is still detectable. As it can be seen, contrarily to the ON1 DLTS peak, the ON2 one shows broad features meaning that it can be due to the overlap of different contributions. In order to resolve them, we employed the following equation:⁹

$$S = \frac{N_T C_{st}}{T_W N_D} (e^{-T_W/\tau} - 1) \frac{2\pi/T_W}{1/\tau^2 + (2\pi/T_W)^2}, \quad (1)$$

where N_T , C_{st} , and T_W are the trap concentration, the steady capacitance under reverse bias condition, and the period width, respectively, while $\tau = \frac{1}{\sigma v_{th} N_C} e^{(E_C - E_T)/kT}$ with σ , v_{th} , N_C , E_T , and k are the capture cross section, thermal velocity, effective density of states, activation energy, and Boltzmann constant, respectively. Fitting of the ON1 peak, by using Eq. (1), reveals an energy position in the bandgap of 0.80 eV, in agreement with the experimental value of 0.79 eV. The simulation of the ON2 level (experimental energy position of $E_C - 1.0 \text{ eV}$) shows that it is indeed due to the overlap of two closely spaced contributions labeled ON2a and ON2b.⁷ As a matter of fact, by using a value of $E_C - 0.96 \text{ eV}$ ($4 \times 10^{-17} \text{ cm}^2$) and $E_C - 0.98 \text{ eV}$ ($9 \times 10^{-18} \text{ cm}^2$) for ON2a and ON2b (red dashed lines), respectively, we could reproduce the ON2 DLTS peak (red solid line).

After 75 min oxidation treatment [Fig. 1(c)], besides the Ti acceptor ($\sim 10^{12} \text{ cm}^{-3}$), ON1 ($4.8 \times 10^{12} \text{ cm}^{-3}$), and ON2 ($1.6 \times 10^{12} \text{ cm}^{-3}$), two new levels labeled OF1 (found at $\sim 115 \text{ K}$) and OF2 ($\sim 175 \text{ K}$), respectively. The reason why OF1 and OF2 have not been reported before may be due to the fact that most FT-DLTS studies did not focus on this temperature range.² As the signal of OF1 and OF2 is rather low, we employed the abovementioned fitting procedure and obtained an energy position in the bandgap of $E_C - 0.19 \text{ eV}$ ($5 \times 10^{11} \text{ cm}^{-3}$) and $E_C - 0.24 \text{ eV}$ ($2 \times 10^{11} \text{ cm}^{-3}$) for OF1 and OF2, respectively.

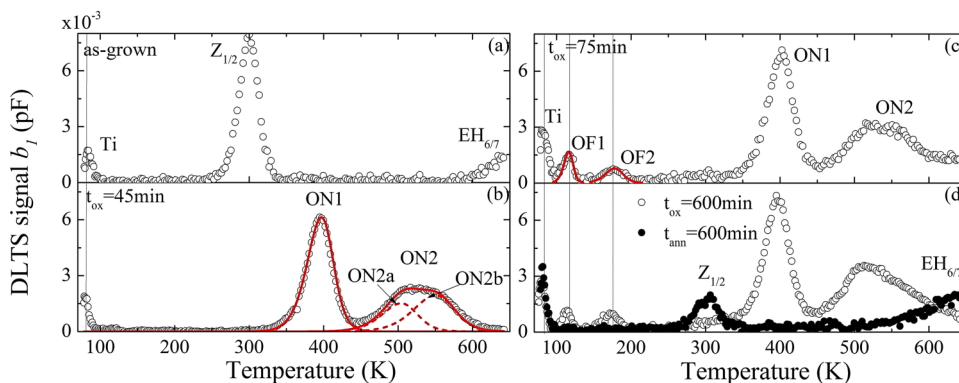


FIG. 1. DLTS spectra of the (a) as-grown, (b) 45 min, (c) 75 min, and (d) 600 min oxidized samples. In (d), the DLTS spectrum of a 600 min annealed sample (filled circles) is shown. Oxidation and annealing are performed at 1290 °C. The period width is set to 0.2 s.

TABLE I. Labeling, energy position in the bandgap (eV), apparent capture cross section (cm^2), and conditions for detection of the levels found in this study. The energy level position and capture cross section of OF1 and OF2 are obtained by employing the fitting procedure described in the text. Oxidation is meant to be dry oxidation process carried out at 1290°C .

| Label | $E_C - E_T$ (eV) | Capture cross section (cm^2) | Comment |
|-------------------|---------------------|--|--------------------------------|
| Ti | 0.16 ± 0.06 | $(1 \pm 0.2) \times 10^{-16}$ | As-grown and oxidized material |
| OF1 | 0.19 ± 0.03 | $(3 \pm 0.06) \times 10^{-17}$ | 75 min oxidized 4H-SiC |
| OF2 | 0.24 ± 0.03 | $(4 \pm 0.08) \times 10^{-19}$ | 75 min oxidized 4H-SiC |
| $Z_{1/2}$ | 0.62 ± 0.02 | $(2 \pm 0.5) \times 10^{-15}$ | As-grown material |
| ON1 | 0.79 ± 0.02 | $(4.7 \pm 0.1) \times 10^{-15}$ | 45 min oxidized 4H-SiC |
| ON2 | 1.0 ± 0.04 | $(1.1 \pm 0.4) \times 10^{-17}$ | 45 min oxidized 4H-SiC |
| $\text{EH}_{6/7}$ | 1.5 ± 0.07 | $(2 \pm 0.7) \times 10^{-15}$ | As-grown material |

Longer oxidation times [600 min, Fig. 1(d)] result in no change of the DLTS spectrum, with the Ti ($7 \times 10^{11} \text{ cm}^{-3}$), OF1 (10^{12} cm^{-3}), OF2 ($8 \times 10^{11} \text{ cm}^{-3}$), ON1 ($5 \times 10^{12} \text{ cm}^{-3}$), and ON2 ($2 \times 10^{12} \text{ cm}^{-3}$) level still detectable. Furthermore, in order to confirm that both OF1 and OF2 are generated by oxidation and are not due to a thermal effect, we annealed the as-grown sample for 600 min at 1290°C in an Ar ambient. Annealing resulted in a spectrum similar to that of Fig. 1(a), with the Ti ($\sim 7 \times 10^{11} \text{ cm}^{-3}$), $Z_{1/2}$, and $\text{EH}_{6/7}$ ($\sim 7.5 \times 10^{11} \text{ cm}^{-3}$) levels present. The decrease in concentration of $Z_{1/2}$ and $\text{EH}_{6/7}$, compared to the nonannealed case, is attributable to the effect reported by Ayedh *et al.*⁶

A summary of the detected traps can be found in Table I.

The 75 min oxidized samples were subsequently annealed at 1600°C for 30 min, in order to verify the thermal stability of OF1 and OF2. Although not shown here, the DLTS spectrum reveals that OF1 and OF2 are thermally stable up to, at least, 1600°C (for 30 min).

In Fig. 2, the depth profiles of the Ti, OF1, OF2, ON1, and ON2 levels are displayed. These were obtained by changing the V_R up to -50 V and by keeping a constant pulse height (2 V). As it can be seen, after 75 min at 1290°C [Fig. 2(a)], the Ti level is rather constant throughout the investigated depth range and the same behavior applies to ON1 and ON2. Instead, OF1 and OF2 have a very similar depth profile and are mainly confined in a region close to the epilayer surface. After longer annealing

[Fig. 2(b)], the depth distribution of Ti is still constant in the investigated depth range, confirming the identification of such level with an extrinsic impurity. The profiles of ON1 and ON2 are also still rather uniform. This might be different to what Kawahara has reported,² that is, the longer the oxidation time, the deeper the distribution of ON1 and ON2 in the epilayer. However, the depth range of our investigation is limited to $\sim 3 \mu\text{m}$, whereas that of Kawahara was much deeper ($15 \mu\text{m}$). On the other hand, after longer oxidation, OF1 and OF2 are distributed $\sim 500 \text{ nm}$ deeper in the epilayer, possibly due to the injection of C_i from the SiO_2/SiC interface, and they still show very similar depth profiles.

Figure 3 shows the effect of postoxidation annealing by N_2O . Nitridation, of a sample oxidized for 45 min at 1290°C , was carried out for 30 min at 1050 or 1290°C . As it can be seen in the figure, nitridation at 1050°C does not have any effect either on the formation or on the concentrations of both ON1 ($5 \times 10^{12} \text{ cm}^{-3}$) and ON2 ($1.4 \times 10^{12} \text{ cm}^{-3}$). However, when N_2O treatment is carried out at 1290°C , OF1 and OF2 can be detected in concentrations similar to those found in the sample oxidized 75 min at 1290°C in the dry atmosphere ($8 \times 10^{11} \text{ cm}^{-3}$ and $6 \times 10^{11} \text{ cm}^{-3}$, respectively), while the concentrations of ON1 and ON2 become $1.6 \times 10^{13} \text{ cm}^{-3}$ and $5 \times 10^{12} \text{ cm}^{-3}$, respectively. Longer nitridation (3 h) does not change the concentrations of both OF1 ($6 \times 10^{11} \text{ cm}^{-3}$) and OF2 ($4 \times 10^{11} \text{ cm}^{-3}$) but increases those of ON1 ($3 \times 10^{13} \text{ cm}^{-3}$) and ON2 (10^{13} cm^{-3}), in agreement with what reported in the literature.²

The similar behavior of OF1 and OF2, with respect to depth distribution and behavior after nitridation, might suggest that these two levels can be related to each other. To prove this, samples were also oxidized at 1222 , 1245 , and 1267°C , for 75 min. The results are plotted in Fig. 4. As it can be seen, both OF1 and OF2 display a one-to-one relation suggesting that they might be two different charge states of the same defect.

For the sake of clarity, we briefly summarize the results reported thus far on OF1 and OF2: (i) they arise only during oxidation ($\geq 75 \text{ min}$), (ii) they possess a rather high thermal stability, (iii) N has no impact on their formation, and (iv) they might be two different charge states of the same defect. We point out that (ii) suggests that, similarly to ON1 and ON2, the microscopic structure of OF1 and OF2 is not related to a single C_i , but rather to a complex one. However, unlike for ON1 and ON2, (iii) excludes

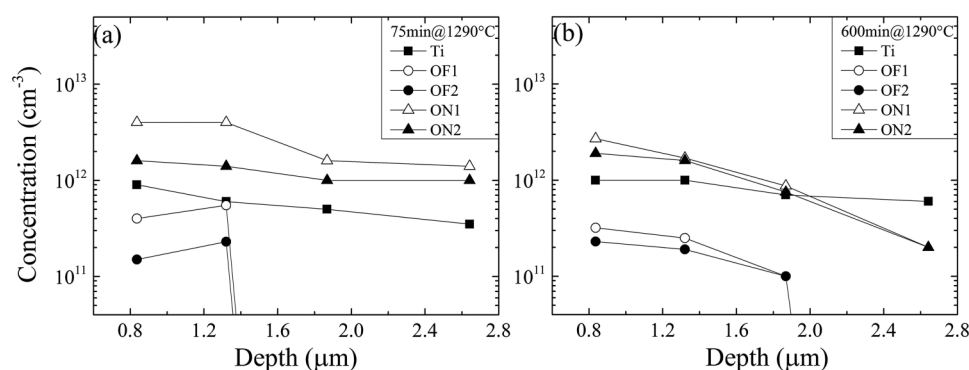


FIG. 2. Depth profiles of Ti, OF1, OF2, ON1, and ON2 after (a) 75 min and (b) 600 min oxidation at 1290°C . The reverse bias was set to -50 V , and the pulse voltage height was kept constant (5 V).

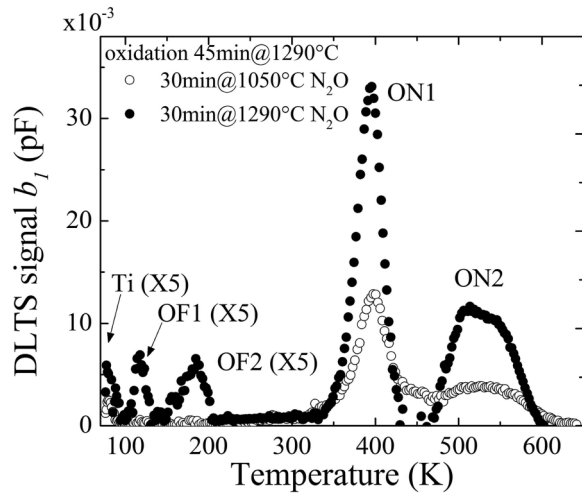


FIG. 3. DLTS spectra of samples oxidized 45 min at 1290 °C and subsequently nitridized for 30 min at 1050 °C or 1290 °C. The period width was set to 0.2 s.

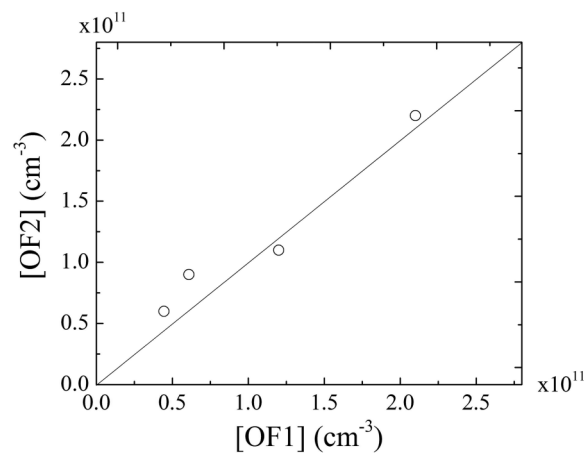


FIG. 4. Plot of the concentration of OF1 vs that of OF2, after oxidation for 75 min at 1222, 1245, 1267, and 1290 °C.

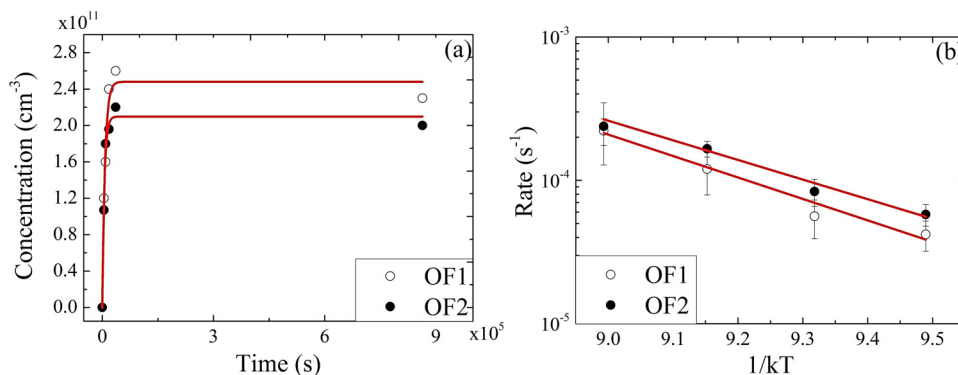


FIG. 5. Plot of the growth of OF1 and OF2. The red solid line is the fit according to Eq. (3). (b) The Arrhenius plot of the generation rates of OF1 and OF2.

the involvement of N in the microscopic structure of OF1 and OF2. For this reason, the hypothesis can be put forward that OF1 and OF2 might be either related to a C_i -related complex (with, e.g., Si) or to a higher order C_i cluster.

In order to gain more insight in the nature of OF1 and OF2, we analyzed their formation kinetics by carrying out an isothermal oxidation series. Four temperatures were selected, 1220, 1245, 1267, and 1290 °C, for times ranging from 75 min to 24 h. We considered the generation of OF1 and OF2 to be regulated by a first-order kinetics,

$$\frac{\partial N(t, T)}{\partial t} = -c(T) \times N(t, T), \quad (2)$$

with $N(t)$ the defect concentration, $c(T)$ the generation constant, and T the absolute temperature. $c(T)$ is defined as $c(T) = c_0 \times \exp(E_a/kT)$, with c_0 and E_a being the pre-exponential factor and the activation energy, respectively.

Figure 5(a) shows the concentrations of OF1 and OF2 as a function of the oxidation time at an oxidation temperature of 1267 °C. It can be seen that the growth of both OF1 and OF2 is described by

$$N(t, T) = N(t, T)^\infty \times (1 - e^{-c(T)t}), \quad (3)$$

with $N(t, T)^\infty$ being the saturated defect concentration, and it is shown as a red solid line. The Arrhenius plot of the generation rates of OF1 and OF2 is shown in Fig. 5(b). From this, we obtained the values of E_a as 3.44 ± 0.4 eV and 3.15 ± 0.2 eV for OF1 and OF2, respectively, whereas the pre-exponential factors are 7×10^9 s $^{-1}$ and 5×10^8 s $^{-1}$ for OF1 and OF2, respectively.

Typically, pre-exponential factors in the 10^{11} – 10^{13} s $^{-1}$ range, indicating that defect generation is due to dissociation of a complex.¹² In the present case, the pre-exponential values are much lower, indicating that the formation of OF1 and OF2 can be due to a reaction between two species A and B. The rate of change in concentration of the defects involved is generally described by

$$-\frac{\partial A}{\partial t} = 4\pi R(D_A + D_B)[A][B] + D_A \frac{\partial^2 A}{\partial t^2}, \quad (4)$$

with R being the capture radius and D_A and D_B the diffusivity of A and B, respectively.

If we consider species B to be more abundant and mobile than A ($[B] \gg [A]$, $D_B \gg D_A$), then Eq. (4) coincides with Eq. (2),

provided that

$$c = 4\pi R D_B [B]. \quad (5)$$

In this context, B is set to be C_i , injected during oxidation. On the other hand, we cannot correlate the generation of the OF1 and OF2 DLTS peak to the annealing of other DLTS peaks. For this reason, we set A as an unknown immobile species.

By setting R as 5 \AA , $[C_i]$ as 10^{12} cm^{-3} , the diffusivity of C_i (D_{C_i}) becomes $1.2 \times 10^8 \text{ cm}^2 \text{ s}^{-1}$ or $8 \times 10^9 \text{ cm}^2 \text{ s}^{-1}$, if we employ the values of E_a and c_0 of OF1 or OF2, respectively. Such calculated values are in quite good agreement with those obtained by Løvlie and Svensson¹² in their study of the annihilation of $Z_{1/2}$ by C_i , confirming that C_i is involved in the nature of both OF1 and OF2.

It now remains to discuss what the nature of this unknown species A would be. This is done by bearing in mind that the defect, resulting from the reaction with C_i , should have two charge states in the upper part of the bandgap and also a rather high thermal stability.

We first consider the hypothesis that A could either be a carbon or a silicon atom. The former gives rise to a carbon split interstitial (C_{sp}), but this option can be discarded as such defect possesses only one charge state in the upper part of the bandgap.¹³ On the other side, the latter case gives rise to a carbon-silicon split interstitial [$(C_{sp})_{Si}$]. This yields two charge states in the upper part of the bandgap¹⁴ but (similarly to C_{sp}) should not be stable at temperatures around 1600°C .¹⁵

Another possibility is A being a C_{sp} or $(C_2)_{Si}$. These defects, acting as a sink for mobile species, lead to the formation of higher order clusters like the tri-interstitial (C_3).¹⁶ However, it was reported that such C_3 should be stable only up to 1200°C .¹⁶

It can also be speculated that species A might be identified as oxygen. It is known that O-donors are relatively close to E_C ,¹⁷ in the same energy range where OF1 and OF2 are found. However, their ionization energy was found to decrease with increasing O incorporation.¹⁷ Furthermore, after incorporating O by either implantation or by growing epilayers in CO_2 ambient, an increase of N_d was reported.¹⁸ Both effects were not observed in the present study.

A more plausible hypothesis is that A is a carbon antisite (C_{Si}). If this is the case, the resulting defect would be a dicarbon antisite [$(C_2)_{Si}$], that is, two carbon atoms sharing a Si-site. Such defect has a rather high dissociation energy (6.7 eV),¹⁵ meaning that it should be stable at very high temperatures and gives rise to four charge states in the bandgap, two of which are in the upper part of the bandgap.

At last, we comment on the possible impact of OF1 and OF2 on the performance of devices. ON1 and ON2, both generated also after oxidation, were found to be weak recombination centers,⁷ and it was concluded that their impact on devices might be small or that they set an upper limit to τ in bulk SiC, achievable by lifetime enhancement techniques.⁷ Although an experimental study on the

impact of OF1 and OF2 on the electronic properties of a device can be subject of a future study, we note that the concentrations of both OF1 and OF2 are typically smaller than those of ON1 and ON2. For this reason, in the case of unipolar devices, such as MOS field effect transistors, the effects on the channel mobility might be small, and, similarly, the impact on τ , in the drift layer of bipolar (p-i-n diodes) devices, would be negligible.

IV. CONCLUSIONS

Dry oxidation performed at 1290°C for at least 75 min showed the formation of two electrically active levels labeled OF1 and OF2, besides the well-known ON1 and ON2. The OF1 and OF2 levels have a high thermal stability, maybe two different charge states of the same defect, and, unlike ON1 and ON2, their concentration is not affected by nitridation. The analysis of the annealing kinetics of OF1 and OF2 revealed that they might arise from the migration of carbon interstitials, which react with some other defect species, possibly a carbon antisite.

REFERENCES

- N. T. Son, X. T. Trinh, L. S. Løvlie, B. G. Svensson, K. Kawahara, J. Suda, T. Kimoto, T. Umeda, J. Isoya, T. Makino, T. Ohshima, and E. Janzén, *Phys. Rev. Lett.* **109**, 187603 (2012).
- K. Kawahara, Ph.D. dissertation, Kyoto University, 2013.
- L. Storasta, H. Tsuchida, T. Miyazawa, and T. Ohshima, *J. Appl. Phys.* **103**, 013705 (2008).
- T. Hiyoshi and T. Kimoto, *Appl. Phys. Express* **2**, 041101 (2009).
- Y. Hijikata, R. Asafuji, R. Konno, Y. Akasaka, and R. Shinoda, *AIP Adv.* **5**, 067128 (2015).
- H. M. Ayedh, R. Nipoti, A. Hallen, and B. G. Svensson, *Appl. Phys. Lett.* **107**, 252102 (2015).
- I. D. Booker, H. Abdalla, J. Hassan, R. Karhu, L. Lilja, E. Janzén, and E. Ö. Sveinbjörnsson, *Phys. Rev. Appl.* **6**, 014010 (2016).
- A. F. Basile, J. Rozen, X. D. Chen, S. Dhar, J. R. Williams, L. C. Feldman, and P. M. Mooney, *ECS Trans.* **28**, 95 (2010).
- S. Weiss and R. Kassing, *Solid State Electron.* **31**, 1733 (1988).
- T. Dalibor, G. Pensl, N. Nordell, and A. Schöner, *Phys. Rev. B* **55**, 13618 (1997).
- E. Omotoso, W. E. Meyer, S. M. M. Coelho, M. Diale, P. N. M. Ngoepe, and F. D. Auret, *Mater. Sci. Semicond. Process.* **51**, 20 (2016).
- L. S. Løvlie and B. G. Svensson, *Phys. Rev. B* **86**, 075205 (2012).
- M. Bockstedte, A. Mattausch, and O. Pankratov, *Phys. Rev. B* **69**, 235202 (2004).
- A. Mattausch, Ph.D. dissertation, Erlangen-Nürnberg University, 2005.
- A. Mattausch, M. Bockstedte, and O. Pankratov, *Phys. Rev. B* **69**, 045322 (2004).
- H. Jiang, C. Jiang, D. Morgan, and I. Szlufarska, *Comp. Mater. Sci.* **89**, 182 (2014).
- T. Dalibor, H. Trageser, G. Pensl, T. Kimoto, H. Matsunami, D. Nizhner, O. Shigiltchhoff, and W. J. Choyke, *Mater. Sci. Eng. B* **61–62**, 454 (1999).
- O. Kletke, G. Pensl, T. Kimoto, and H. Matsunami, *Mater. Sci. Forum* **353–356**, 459 (2001).